



**Exploiting satellite measurements to reduce uncertainties in  
UK bottom-up NO<sub>x</sub> emission estimates**

Richard J. Pope<sup>1,2</sup>, Rebecca Kelly<sup>1</sup>, Eloise A. Marais<sup>3</sup>, Ailish M. Graham<sup>1</sup>,  
Chris Wilson<sup>1,2</sup>, Jeremy J. Harrison<sup>4,5</sup>, Savio J. A. Moniz<sup>6</sup>, Mohamed Ghalaïeny<sup>6</sup>, Steve R.  
Arnold<sup>1</sup> and Martyn P. Chipperfield<sup>1,2</sup>

*1: School of Earth and Environment, University of Leeds, Leeds, UK*

*2: National Centre for Earth Observation, University of Leeds, Leeds, UK*

*3: Department of Geography, University College London, London, UK*

*4: Department of Physics and Astronomy, University of Leicester, Leicester, UK*

*5: National Centre for Earth Observation, University of Leicester, Leicester, UK*

*6: Department for Environment, Food and Rural Affairs, 2 Marsham Street, London, UK*

*Correspondence to:* Richard J. Pope (r.j.pope@leeds.ac.uk)

**Abstract**

Nitrogen oxides (NO<sub>x</sub>, NO+NO<sub>2</sub>) are potent air pollutants which directly impact on human health and which aid the formation of other hazardous pollutants such as ozone (O<sub>3</sub>) and particulate matter. In this study, we use satellite tropospheric column nitrogen dioxide (TCNO<sub>2</sub>) data to evaluate the spatiotemporal variability and magnitude of the United Kingdom (UK) bottom-up National Atmospheric Emissions Inventory (NAEI) NO<sub>x</sub> emissions. Although emissions and TCNO<sub>2</sub> represent different quantities, for UK city sources we find a spatial correlation of ~0.5 between the NAEI NO<sub>x</sub> emissions and TCNO<sub>2</sub> from the high-spatial-resolution TROPospheric Monitoring Instrument (TROPOMI), suggesting a good spatial distribution of emission sources in the inventory. Between 2005 and 2015, the NAEI total UK NO<sub>x</sub> emissions and long-term TCNO<sub>2</sub> record from the Ozone Monitoring Instrument (OMI), averaged over England, show decreasing trends of 4.4% and 2.2%, respectively. Top-down NO<sub>x</sub> emissions were derived in this study by applying a simple mass balance approach to TROPOMI observed downwind NO<sub>2</sub> plumes from city sources. Overall, these top-down estimates were consistent with the NAEI, but for larger cities such as London and Manchester the inventory is significantly (>25%) less than the top-down emissions. This NAEI NO<sub>x</sub> emission underestimate is supported by comparing simulations from the GEOS-Chem atmospheric chemistry model, driven by the NAEI emissions, with satellite and surface NO<sub>2</sub> observations over the UK. This yields substantial model negative biases, providing further evidence to demonstrate that the NAEI may be underestimating NO<sub>x</sub> emissions in London and Manchester.



## 1. Introduction

Poor air quality (AQ) can have a substantial impact on human health, increasing risk of ailments such as asthma, cancer, diabetes and heart disease (Royal College of Physicians, 2016). A key air pollutant is nitrogen dioxide ( $\text{NO}_2$ ) which was responsible for approximately 9600 premature deaths from long-term exposure in the UK in 2015 (EEA, 2018).  $\text{NO}_2$  is also a precursor to tropospheric ozone and nitrate aerosol in the UK (DEFRA, 2018a). Legislation (e.g. the EU directive 2008/50/EC Ambient AQ regulation, (DEFRA, 2018a)) is in place to reduce concentrations of  $\text{NO}_2$  and other pollutants. However, many regions in the UK (33 out of 43 in 2019; DEFRA, 2020) still fail to meet the annual mean  $\text{NO}_2$  limit of  $40 \mu\text{g}/\text{m}^3$  (WHO, 2018). To meet the UK's statutory reporting requirements and to help inform policy, Defra uses the National Atmospheric Emissions Inventory (NAEI, 2021). However, like all emission inventories, the NAEI is subject to uncertainties which are difficult to quantify. These uncertainties include unreported sources, diffuse sources such as agriculture, the use of proxy data (e.g. population or housing density data) to distribute emissions and updates to the NAEI methodologies between years (NAEI, 2017). In addition, the NAEI only includes emissions from anthropogenic sources. Spatial verification of NAEI AQ emissions is restricted to comparisons with surface sites, which have limited and disproportional spatial coverage. The NAEI is also used to drive regional models (e.g. the UK Met Office Air Quality in the Unified Model (AQUM, Savage et al., 2013) which provides the official national AQ forecasts), land use regression models (e.g. Wu et al., 2017) and Pollutant Climate Mapping (PCM) models (e.g. Dibbens and Clemens, 2015), where uncertainties in the emissions can then feed into the simulated AQ predictions and resultant public health advisories.

Satellite measurements of tropospheric column  $\text{NO}_2$  ( $\text{TCNO}_2$ ) have frequently been used to derive top-down emissions of nitrogen oxides ( $\text{NO}_x$  = nitric oxide (NO) +  $\text{NO}_2$ ), which can be used to evaluate bottom-up inventories. Some studies have used statistical fitting of observed downwind plumes of  $\text{TCNO}_2$  from anthropogenic sources (e.g. Beirle et al., 2011; Liu et al., 2016; Verstraeten et al., 2018), while others have used complex atmospheric chemistry models deploying approaches such as data assimilation (e.g. Miyazaki et al., 2016), mass balance (Martin et al., 2003) and model sensitivity experiments (e.g. Potts et al., 2021).

While model-derived estimates of  $\text{NO}_x$  emissions (e.g. from data assimilation) are robust, the methodology is computationally expensive and time intensive. Therefore, the statistical fitting to downwind plumes approach is a more achievable approach to derive top-down emissions, especially for government departments and agencies. Beirle et al. (2011) presented one of the first studies to use statistical fitting to downwind plumes for Riyadh, Saudi Arabia. The method was also applied to multiple megacities and compared with the bottom-up Environmental Database for Global Atmospheric Research (EDGAR) emission inventory (version 4.1). Verstraeten et al. (2018) used a similar, but modified, approach of a simple mass balance which assumes that the observed total mass of  $\text{NO}_2$  is a product of the emission rate and the effective lifetime. The assumption is that the removal of  $\text{NO}_2$  can be described by a first-order loss (i.e. the chemical decay of  $\text{NO}_2$  follows an exponential decay function with an e-folding time, and therefore distance from source).

In this study, we use satellite  $\text{TCNO}_2$  records to evaluate the spatial distribution and temporal evolution of the NAEI. We apply a similar approach to Verstraeten et al. (2018), but determine the background  $\text{NO}_2$  value and e-folding distance in different ways, to derive top-down  $\text{NO}_x$  emission estimates of UK cities and thereby directly evaluate the NAEI estimates. This work



represents the first attempt to derive UK city-scale  $\text{NO}_x$  emissions from the new state-of-the-art TROPospheric Monitoring Instrument (TROPOMI), which has unparalleled spatial resolution in comparison to previous sensors (e.g. the Ozone Monitoring Instrument, OMI). Therefore, we can derive  $\text{NO}_x$  emissions from previously undetectable sources (e.g. Manchester and Birmingham). From here on, we refer to this methodology as the simple mass balance approach (SMBA). The satellite observations used, NAEI and SMBA are described in Section 2, the results presented in Section 3 and our conclusions discussed in Section 4.

## 2. Data and Methods

### 2.1 NAEI Emissions

The NAEI is the official UK bottom-up inventory of primary sources of emissions, used for statutory reporting, national air quality policy and driving regional air quality models (NAEI, 2021). The contract to deliver the NAEI is led by a consortium managed by Ricardo Energy and Environment for the UK Department for Business, Energy and Industrial Strategy (BEIS) and the Department for Environment, Food and Rural Affairs (Defra). The NAEI is compiled on an annual basis according to internationally agreed methodologies (EMEP/EEA, 2019), encompassing sectors ranging from transport, industry, through to agriculture and domestic sources (Ricardo Energy and Environment, 2021). Here, we use the NAEI emissions from 2016 as this was the most recent dataset available when this work started and used in computationally time consuming model simulations (see Section 3.4). The most recent year now available is 2019. For comparison to top-down emissions estimates (see Section 3.3), using average  $\text{TCNO}_2$  data centred on 2019, we extrapolate the NAEI 2016 emission values to 2019 levels for a more representative temporal comparison. The extrapolation was based on a simple linear trend ( $-3.9\%/yr$ ) for the NAEI UK  $\text{NO}_x$  total emissions between 2009 and 2018 (i.e. 10 years) and imposed on the NAEI 2016 gridded emissions.

### 2.2 Satellite Data

OMI and TROPOMI are both nadir-viewing instruments on-board the NASA Aura and ESA Sentinel 5 – Precursor (S5P) polar orbiting satellites, respectively, and have local overpass times of 13:30. TROPOMI measures in the ultraviolet-visible (UV-Vis, 270-500 nm), similar to OMI (Boersma et al., 2007), as well as near-infrared (NIR, 675-775 nm) and short-wave infrared (SWIR, 2305-2385 nm) spectral ranges (Veefkind et al., 2012). TROPOMI and OMI have nadir pixel sizes of  $3.5 \text{ km} \times 5.5 \text{ km}$  (in the UV-Vis,  $7.0 \text{ km} \times 7.0 \text{ km}$  for other spectral ranges) and  $13 \text{ km} \times 24 \text{ km}$ , respectively. The OMI (DOMINO version 2 product) and TROPOMI (TM5-MP-DOMINO version 1.2/3x – OFFLINE product) data were downloaded from the Tropospheric Emissions Monitoring Internet Service (TEMIS) for January 2005 to December 2015 and February 2018 to January 2020, respectively. We did not consider OMI  $\text{TCNO}_2$  after 2015 as the row anomaly substantially degraded the quality of the data over the UK from this point. The data has been processed using the methodology of Pope et al., (2018) to map the  $\text{TCNO}_2$  data onto a high-resolution spatial grid ( $0.025^\circ \times 0.025^\circ$ ,  $\sim 2\text{-}3 \text{ km} \times \sim 2\text{-}3 \text{ km}$  for TROPOMI,  $0.05^\circ \times 0.05^\circ$ ,  $\sim 5 \text{ km} \times \sim 5 \text{ km}$  for OMI). The TROPOMI data were quality controlled for a cloud radiance fraction  $< 0.5$ , a quality control flag  $> 50$  and where the  $\text{TCNO}_2$  value was  $> -1.0 \times 10^{-5} \text{ moles/m}^2$  (i.e. random values round 0.0 may be slightly negative or positive so we filter for  $\text{TCNO}_2 > -1.0 \times 10^{-5} \text{ moles/m}^2$  otherwise a positive bias in average  $\text{TCNO}_2$  is imposed).



While TROPOMI provides the greatest spatial resolution of any satellite instrument to measure air pollutants, suitable to derive TCNO<sub>2</sub> emission estimates over UK city-scale sources, the retrieved TCNO<sub>2</sub> has been shown to have a low bias. Over north-western Europe, Verhoelst et al., (2021) found that TROPOMI underestimated TCNO<sub>2</sub> by approximately 20–30% when compared with surface TCNO<sub>2</sub> measurements, which is consistent with Chan et al., (2020) and Dimitropoulou et al., (2020). OMI data were processed for a geometric cloud fraction of <0.2, quality flag = 0 (which also flags pixels influenced by the row anomaly (Braak, 2010)) and TCNO<sub>2</sub> > -1.0×10<sup>-5</sup> moles/m<sup>2</sup>.

### 2.3 Simplified Mass Balance Approach

To derive top-down emissions of NO<sub>2</sub> we use the SMBA, which is based on downwind plumes of TROPOMI observed TCNO<sub>2</sub> from the target source where the observed total mass of NO<sub>2</sub> (i.e. the source-related enhancement of TCNO<sub>2</sub> above the background level) is assumed to be a product of the emission rate and the effective lifetime. Therefore, we can derive the emission rate based on **Equation 1**:

$$E = \frac{\sum_{i=0}^N (NO_2 LD_i \times \Delta d)}{t \times e^{-\frac{t}{\tau}}} \quad (1)$$

where  $E$  is the emission rate (moles/s),  $NO_2 LD$  is the NO<sub>2</sub> line density (moles/m),  $\Delta d$  is the grid box length (m),  $i$  is the grid box number between the source and background value,  $t$  is time (s) and  $e^{-\frac{t}{\tau}}$  is the e-folding loss term with  $\tau$  as the effective lifetime.  $N$  represents the number of satellite TCNO<sub>2</sub> grid boxes between the source and background level  $B$ .  $t$  is calculated as the distance between the source and  $B$  divided by the wind speed ( $ws$ ). The wind speed and direction at a particular source are determined from the European Centre for Medium-Range Weather Forecasts (ECMWF) ERA5  $u$ - &  $v$ -wind component data. The wind data are sampled at 13:00 UTC (around 13:00 local solar time over the UK) to coincide with the TROPOMI overpass (i.e. 13:30 local solar time, LST) and averaged across boundary layer pressure levels (i.e. 1000 hPa and 850 hPa). In all cases,  $ws$  had to be greater than 2 m/s to avoid near stable meteorological conditions. **Figure 1a** shows the difference between TROPOMI TCNO<sub>2</sub> sampled under westerly flow and the long-term average based on London  $u$ - and  $v$ -wind components. The  $NO_2 LD$  is the product of the source width, which is perpendicular to the wind flow, and the source-width-average TCNO<sub>2</sub> profile downwind from the source. The TCNO<sub>2</sub> profile is the cross-section between the grid box the source centre is located in and the grid box where  $B$  is reached with units of moles/m<sup>2</sup>. As there may be several downwind TCNO<sub>2</sub> profiles within the source width, these are averaged together to form an average downwind profile across the source width. As the source emissions will be a function of the source width (i.e. larger in source centre and lower at source edge), the mean TCNO<sub>2</sub> downwind profile is most representative of source-average NO<sub>2</sub> emission.

As shown in **Figure 1b**, the downwind plume (e.g. westerly flow over London) has typically larger  $NO_2 LD$  values than the all-flow (i.e. all wind directions)  $NO_2 LD$ . The full NO<sub>2</sub> mass emitted from the source in the  $NO_2 LD$  is the summation of the wind-flow  $NO_2 LD$  from source up to point  $B$ . A reasonable estimate of when the wind-flow  $NO_2 LD$  reaches  $B$  is when it intersects with the all-flow  $NO_2 LD$  profile (i.e. returns to normal levels). However, when there are substantial upwind NO<sub>2</sub> sources, this can yield wind-flow  $NO_2 LD$  profiles which never intersect with the all-flow  $NO_2 LD$  profile within the domain (e.g. see Birmingham example in



190 **Figure 2a & b).** Therefore, to determine when  $B$  has been reached, a running t-test was  
 191 applied to the wind-flow  $\text{NO}_2$  LD profile to determine where turning points or levelling off  
 192 occurred. As such a test can be sensitive to noise in the  $\text{TCNO}_2$  data, a 10-pixel ( $0.5^\circ$ ) running  
 193 average wind-flow  $\text{NO}_2$  LD profile was calculated. The running t-test was applied to this using  
 194 two windows of the same size to identify step changes in the profile. The green line in **Figure**  
 195 **1b** shows where the t-test p-value has become large and there is a turning point in the wind-  
 196 flow  $\text{NO}_2$  LD profile. Such a reduction in the wind-flow  $\text{NO}_2$  LD profile gradient is suggestive  
 197 of the plume reaching  $B$  as  $\text{NO}_2$  levels have stabilised. However, in **Figure 1b**, there are  
 198 multiple locations potentially meeting this criteria. In reality, the turning points further  
 199 downwind of London are sources from the Benelux region. The red dot represents the first  
 200 instance, after the initial near-source wind-flow  $\text{NO}_2$  LD peak, where the gradient in the  
 201 running t-test p-value profile changes sign (i.e. positive to negative or vice versa). The wind  
 202 flow  $\text{NO}_2$  LD then has the background  $\text{NO}_2$  LD value subtracted from all points between the  
 203 source and  $B$  and is then summed yielding the total  $\text{NO}_2$  mass (moles).

204 The loss term  $e^{-\frac{t}{\tau}}$  is dependent upon  $\tau$  and is determined by applying an e-folding distance fit  
 205 between the near-source peak wind-flow  $\text{NO}_2$  LD value and  $B$ , before dividing by  $ws$  to get  $\tau$ .

206 Here, a range of e-folding distances are tested in the loss term  $e^{-\frac{t}{\tau}}$  to find the distance value  
 207 which yields the lowest root mean square error (RMSE), and a large  $R^2$  (Pearson correlation  
 208 coefficient squared) value, between the e-folding distance fit (red line, **Figure 1c**) and the  
 209 wind-flow  $\text{NO}_2$  LD (black line, **Figure 1c**). In the case of London, this yielded an e-folding  
 210 distance of 150.0 km and  $\tau$  of 3.8 hours (7.0 and 2.6 hours) based on  $ws = 9.9 \text{ m/s}$  ( $\pm 4.6 \text{ m/s}$ ;  
 211 i.e.  $\pm 1$ -sigma standard deviation). The effective lifetime derived here for London and other  
 212 UK cities is typically consistent with values from other studies (e.g. Beirle et al., (2011) and  
 213 Verstraeten et al. (2018)) for European cities (i.e. 1.0–10.0 hours).

214  
 215 The top-down  $E$  is calculated from **Equation 1**, but this is an emissions flux of  $\text{NO}_2$  moles/s  
 216 which needs to be converted to  $\text{NO}_x$  for comparison with the bottom-up inventories. This is  
 217 done by scaling the  $\text{NO}_2$  emissions by 1.32 based on the  $\text{NO}:\text{NO}_2$  concentration ratio (0.32) in  
 218 urban environments at midday (Seinfeld and Pandis, 2006; Liu et al., 2016). Verstraeten et al.,  
 219 (2018) used modelled  $\text{NO}$  and  $\text{NO}_2$  concentrations to derive a scaling more representative of  
 220 the chemistry of the source. They estimate there is a 10% uncertainty (similar to Beirle et al.,  
 221 (2011)), but as the modelled  $\text{NO}_2:\text{NO}_x$  ratio is based on the input emissions, for which the  
 222 satellite data is being used to evaluate, this process is rather circular and not independent.  
 223 The final emission uncertainty estimates (**Figure 1**) are derived by  $\pm$  the satellite error ( $10^{-5}$   
 224 moles/ $\text{m}^2$ ) before obtaining the  $\text{NO}_2$  LD (Sat  $\text{NO}_x$  Emissions-1) and by using the uncertainties  
 225 in  $\tau$  when determining the loss term (Sat  $\text{NO}_x$  Emissions-2).

## 226 227 **2.4 GEOS-Chem Model**

228  
 229 To help evaluate the robustness of our derived top-down SMBA  $\text{NO}_x$  emissions, we use the  
 230 comprehensive, state-of-the-science GEOS-Chem chemical transport model. GEOS-Chem has  
 231 emissions inputs from the NAEI and therefore comparison of the model with  $\text{NO}_2$   
 232 observations can be used as test of the NAEI. Therefore, if there are inconsistencies between  
 233 the SMBA and NAEI  $\text{NO}_x$  emissions, which correspond to model – observational differences,  
 234 this supports the robustness of the SMBA emission methodology. Simulations from the GEOS-  
 235 Chem version used here are described in Potts et al. (2021) (version 12.1.0;



https://doi.org/10.5281/zenodo.1553349) and are run using the NAEI 2016 emissions but scaled to expected 2019 levels. The model has been run between January and June representing half the seasonal cycle (i.e. peak to trough in the NO<sub>2</sub> seasonal cycle), so this 6-month average should be suitably representative of the annual average. The model is nested over Europe (32.75-61.25°N, 15°W-40°E) at a 0.25° latitude × 0.3125° longitude horizontal resolution. The model vertical domain extends from the surface to 0.01 hPa. The model is driven with NASA Global Modelling and Assimilation Office (GMAO) Goddard Earth Observing System – Forward Processing (GEOS-FP) assimilated meteorology. Dynamic (3-hourly) boundary conditions are from a global version of the model simulated at 4° latitude × 5° longitude. The model includes detailed gas-phase chemistry, aerosol processes and wet and dry deposition. Anthropogenic emissions for the UK are from the NAEI and continental emissions are from the European Monitoring and Evaluation Programme (EMEP) inventory (EMEP, 2021). Natural emissions from soils and lightning are included.

For comparisons with TROPOMI TCNO<sub>2</sub>, the model is output (averaged between 12:00 – 15:00 LST) around the overpass of the satellite (~13:30 LST) and spatially co-located with the satellite swaths to reduce representation errors in any comparisons. The smoothing errors (i.e. where the instrument is vertically sensitive to retrieving NO<sub>2</sub>) are accounted for with the satellite averaging kernels (AK).

Once a model vertical profile has been co-located with the satellite retrieval (i.e. a pixel in the satellite swath which has passed the quality control filters), the model profile is interpolated in  $\log(\text{pressure})$  onto the satellite vertical grid. The model sub-columns are then derived using the hydrostatic balance approximation:

$$\text{mass density} = \text{mmr} \times \rho dz = \text{mmr} \times \frac{-dp}{g} \quad (2)$$

where *mass density* is mass (kg) of NO<sub>2</sub> per m<sup>2</sup> between two pressure levels, *mmr* is the NO<sub>2</sub> mass mixing ratio from the model,  $\rho$  is the density, *dz* is the distance between pressure levels, *dp* is the pressure difference between levels and *g* is the acceleration due to gravity (-9.81 m/s<sup>2</sup>). The tropospheric AK is then applied to the model sub-column profile as follows:

$$\text{Model TCNO}_2 = \frac{\text{AMF}}{\text{AMF}_{\text{trop}}} \times \sum_{i=0}^{\text{trop lev}} \text{AK}_i \times \text{mass density}_i \quad (3)$$

where *Model TCNO<sub>2</sub>* (kg/m<sup>2</sup>) is the model TCNO<sub>2</sub> with the AK applied, *AMF* is the air mass factor, *AMF<sub>trop</sub>* is the troposphere air mass factor, *i* the vertical sub-column number, *trop lev* is the index of the vertical grid box in which the troposphere occurs and *AK* is the averaging kernel. *Model TCNO<sub>2</sub>* is then converted to moles/m<sup>2</sup> for comparisons with TROPOMI TCNO<sub>2</sub>. GEOS-Chem is also compared with NO<sub>2</sub> data from the surface Automatic Urban and Rural Network (AURN, 2021) (using urban background, suburban and rural) sites over the same time period (January to June, 2019) and sampled at 13:00 LST to match the TROPOMI overpass time.



### 3. Results

#### 3.1 NO<sub>x</sub> Sources

Surface emissions and observed TCNO<sub>2</sub> represent different quantities and are influenced by different processes. However, the short NO<sub>2</sub> lifetime of a few hours (Schaub et al., 2007; Pope et al., 2015) means there is a sharp gradient between sources and the background levels. Therefore, we can use the satellite TCNO<sub>2</sub> observations to provide some constraint on the spatial distribution of the NO<sub>x</sub> emissions. In **Figure 3**, spatial maps over south-eastern (**Figure 3a & c**) and northern England (**Figure 3b & d**) show evidence of co-located TCNO<sub>2</sub> and NO<sub>x</sub> emission hot spots, especially over many of the UK cities shown by circles. Here, both data sets have been mapped onto the spatial resolution of 0.025° × 0.025°. In South East England, TCNO<sub>2</sub> and NO<sub>x</sub> emissions peak over London at over 14.0 × 10<sup>-5</sup> moles/m<sup>2</sup> and approximately >2.0 µg/m<sup>2</sup>/s, respectively. A secondary peak is also observed over western London for both quantities at similar levels. There are further co-located hotspots over Southampton (TCNO<sub>2</sub> ~8.0-9.0 × 10<sup>-5</sup> moles/m<sup>2</sup>, NO<sub>x</sub> >2.0 µg/m<sup>2</sup>/s), Portsmouth (TCNO<sub>2</sub> ~6.0-7.0 × 10<sup>-5</sup> moles/m<sup>2</sup>, NO<sub>x</sub> ~1.0-1.5 µg/m<sup>2</sup>/s), Brighton (TCNO<sub>2</sub> ~5.0-6.0 × 10<sup>-5</sup> moles/m<sup>2</sup>, NO<sub>x</sub> ~0.5-0.8 µg/m<sup>2</sup>/s), Oxford (TCNO<sub>2</sub> ~7.0-7.5 × 10<sup>-5</sup> moles/m<sup>2</sup>, NO<sub>x</sub> ~0.7-1.0 µg/m<sup>2</sup>/s) and Chelmsford (TCNO<sub>2</sub> ~8.5-9.5 × 10<sup>-5</sup> moles/m<sup>2</sup>, NO<sub>x</sub> ~0.5 µg/m<sup>2</sup>/s). In northern England and the Midlands, peak TCNO<sub>2</sub> and NO<sub>x</sub> emissions are located over Manchester (TCNO<sub>2</sub> ~10.0-11.0 × 10<sup>-5</sup> moles/m<sup>2</sup>, NO<sub>x</sub> ~1.0-1.5 µg/m<sup>2</sup>/s), Birmingham (TCNO<sub>2</sub> ~8.0-9.0 × 10<sup>-5</sup> moles/m<sup>2</sup>, NO<sub>x</sub> ~1.0-1.5 µg/m<sup>2</sup>/s), Leeds (TCNO<sub>2</sub> ~8.0-9.0 × 10<sup>-5</sup> moles/m<sup>2</sup>, NO<sub>x</sub> ~1.0-1.5 µg/m<sup>2</sup>/s) and Liverpool (TCNO<sub>2</sub> ~7.0-8.0 × 10<sup>-5</sup> moles/m<sup>2</sup>, NO<sub>x</sub> ~0.5-1.0 µg/m<sup>2</sup>/s).

To quantify the spatial relationship between the TCNO<sub>2</sub> and NO<sub>x</sub> emissions over source regions, the corresponding pixels of both data sets were sub-sampled for each UK city (79 in total), normalised by the sample mean and correlated against each other (red circles, **Figure 3e**), which yielded a correlation  $R_{city1 \times 1} = 0.38$  (i.e. city1 × 1 represents 1 grid box × 1 grid box or 0.025° × 0.025° around where the city centre is located). However, as atmospheric NO<sub>2</sub> is subject to chemical reactions and meteorological processes (e.g. transport), the signal around source regions is more diluted and the peak TCNO<sub>2</sub> not necessarily centred on the source. To allow for that, the spatial resolution of the quantities over each source was degraded, averaging over 3 × 3 (**Figure 3f**), 5 × 5 (**Figure 3g**) and 7 × 7 (**Figure 3h**) grid cells and the correlation recalculated (e.g. city3 × 3 represents 3 grid box × 3 grid box or 0.075° × 0.075° around where the city centre is located). This resulted in correlations of  $R_{city3 \times 3} = 0.51$ ,  $R_{city5 \times 5} = 0.58$  and  $R_{city7 \times 7} = 0.52$ . The correlation for full domain (i.e. the UK) was  $R_{all} = 0.14$ . As expected, the correlation for all grid pixels (e.g. including pixels over the sea) is weak where long-range transport of NO<sub>2</sub> can yield spatial variability in background regions with corresponding zero emission pixels. The  $R_{city1 \times 1}$ ,  $R_{city3 \times 3}$ ,  $R_{city5 \times 5}$  and  $R_{city7 \times 7}$  correlations were all larger. The largest city-scale correlation was for the  $R_{city5 \times 5}$  values where the spatial variability has been smoothed and is representative of the more diffuse pattern of TCNO<sub>2</sub>. However, the  $R_{city7 \times 7}$  (0.175° × 0.175° or ~15-20 km × 15-20 km) correlation is lower than the  $R_{city5 \times 5}$  value suggesting that this scale is larger than most UK city sizes. Overall, for all R values, except for  $R_{all}$ , there are statistically significant positive correlations at the 90% confidence level (CL) or above (>95% CL for  $R_{city3 \times 3}$ ,  $R_{city5 \times 5}$  and  $R_{city7 \times 7}$ ). Therefore, the city-scale emission-satellite correlations provide confidence in the spatial distribution of the NAEI NO<sub>x</sub> emissions based on the observed satellite TCNO<sub>2</sub>.



### 3.2 Satellite NO<sub>2</sub> and Emission NO<sub>x</sub> Trends

To evaluate the temporal evolution of the NAEI emissions, we use the long-term satellite record of TCNO<sub>2</sub> from OMI between 2005 and 2015. Annual total UK emissions of NO<sub>x</sub> (treated as NO here) from the NAEI start in 1970 and continue to present day (typically with a lag of approximately two years). Annual spatial maps of the NAEI also exist over the same time period. However, while there is a consistent methodology for the UK total estimates, the mapping methodology updates between years (NAEI, 2017). Therefore, instead of performing trends on the maps, we focus on trends in the UK NO<sub>x</sub> emission totals. For OMI, we have taken a similar broad scale approach focussing on averaged TCNO<sub>2</sub> across England (defined as 3°W–2°E, 50–54°N). We focus on England as the majority of large UK sources with reasonable spatiotemporal coverage are located here and have clearly defined trends over source regions. Pope et al., (2018) showed significantly (at the 95% CL) decreasing trends over London, Birmingham, Manchester and the Yorkshire power stations of between 1.5% and 2.3% per year. OMI measurements can be subject to large uncertainties and variability, so this analysis also investigates trends in a range of OMI TCNO<sub>2</sub> percentiles over time. To estimate the annual absolute England total NAEI NO<sub>x</sub> emissions, we summed the emissions data for England (same geographical definition as for OMI above) from the 2016 NAEI NO<sub>x</sub> emissions map and imposed the UK total NO<sub>x</sub> trend on it. Here, we use a simple linear fit which yields an annual decrease in the UK total NO<sub>x</sub> emission of 4.4%. The relative rate of change is the same for the England total NO<sub>x</sub> emissions, but the absolute values are lower than the UK total NO<sub>x</sub> emissions (**Figure 4, top panel**).

Over the 2005–2015 period, the England average OMI TCNO<sub>2</sub> trends in the 10<sup>th</sup>, 25<sup>th</sup>, 50<sup>th</sup>, 75<sup>th</sup> and 90<sup>th</sup> percentiles are  $-0.18 \times 10^{-5}$  moles/m<sup>2</sup>/yr (–3.3%/yr),  $-0.20 \times 10^{-5}$  moles/m<sup>2</sup>/yr (–2.7%/yr),  $-0.21 \times 10^{-5}$  moles/m<sup>2</sup>/yr (–2.2%/yr),  $-0.17 \times 10^{-5}$  moles/m<sup>2</sup>/yr (–1.3%/yr) and  $-0.07 \times 10^{-5}$  moles/m<sup>2</sup>/yr (–0.4%/yr), respectively (**Figure 4**). All of the satellite trends are significant at the 95% CL except for the 90<sup>th</sup> percentile. The UK and England total NO<sub>x</sub> emission trends between 2005 and 2015 are –49.7 kt/yr and –30.1 kt/yr (both –4.4%/yr). The OMI TCNO<sub>2</sub> trends range between –3.2% and –0.4% depending on the data percentile used to generate the average England TCNO<sub>2</sub> annual time series. We also calculated annual trends in UK and England (same definition as above) surface NO<sub>2</sub> observations (**Figure 4, bottom panel**) from AURN (AURN, 2021). Here, we used urban background, suburban and rural sites. For the 10<sup>th</sup>, 25<sup>th</sup>, 50<sup>th</sup>, 75<sup>th</sup> and 90<sup>th</sup> percentiles, UK (England) trends are –0.26 (–0.27) µg/m<sup>3</sup>/yr, –0.40 (–0.52) µg/m<sup>3</sup>/yr, –0.73 (–0.77) µg/m<sup>3</sup>/yr, –0.95 (–0.95) µg/m<sup>3</sup>/yr and –1.19 (–1.09) µg/m<sup>3</sup>/yr. This corresponds to –3.77 (–3.03) %/yr, –3.07 (–3.24) %/yr, –3.03 (–2.86) %/yr, –2.49 (–2.31) %/yr and –2.29 (–1.98) %/yr. Therefore, the NAEI NO<sub>x</sub> emissions trend is of similar magnitude and direction to that of the observations. The differences are most likely explained by the non-linear conversion of emissions to atmospheric concentrations (i.e. complex meteorology and chemistry). The likely drivers for decreases in UK NO<sub>x</sub> emissions and NO<sub>2</sub> concentrations include a shift to cleaner energy sources (e.g. National Emissions Ceilings Regulations 2018, DEFRA, (2018b)), regulations on industrial and power generation emissions (Environmental Permitting Regulations 2016 (UK Government, 2016)) and tighter emissions for vehicles (e.g. Euro 6 emissions standards). Overall, these results provide confidence in the use of the satellite data as a tool to evaluate bottom-up emissions trends.



### 3.3 Top-Down NO<sub>x</sub> Emissions

The top-down NO<sub>x</sub> emission rate for London under westerly flow (**Figure 1**) is 58.7 moles/s (37.7, 79.8 moles/s, based on Sat NO<sub>x</sub> Emissions-1 uncertainties), while the NAEI flux is 32.7 moles/s. Here, the NAEI has a low bias with the top-down estimate and sits outside the uncertainty range. The top-down emissions are based on 2 years, so the flux should be representative of an annual emission rate, corresponding to the NAEI reporting. In the case of Birmingham (**Figure 2a**), under easterly flow, there is a visible plume (i.e. positive differences of  $2.0\text{--}3.0 \times 10^{-5}$  moles/m<sup>2</sup>) superimposed on a background enhancement ( $0.5\text{--}1.0 \times 10^{-5}$  moles/m<sup>2</sup>). As a result, the wind-flow NO<sub>2</sub> LD is always larger than the all-flow NO<sub>2</sub> LD and never reaches the background level (i.e. zero differences in **Figure 2a**) within the domain for which the TROPOMI TCNO<sub>2</sub> data has been processed for (e.g. there are positive differences in between the source, Birmingham, and the west of the domain, 8°W). Therefore, the running t-test methodology is used to determine when the wind-flow NO<sub>2</sub> LD reaches a steady background state *B*, as shown in **Figure 2b**. Overall, the NAEI (14.8 moles/s) underestimates the top-down emissions for Birmingham under easterly flow (27.3 (17.8, 36.9) moles/s).

Our methodology was applied to 12 city sources where sources had suitable downwind TCNO<sub>2</sub> enhancements to derive NO<sub>2</sub> LDs and top-down emissions (**Figure 5**). These are shown in **Table 1**. Where top-down emissions could be derived for sources over several wind directions, they were averaged together. The TCNO<sub>2</sub> response to mesoscale and synoptic weather systems (i.e. large scale flow) can be seasonally influenced (e.g. Pope et al., 2015) with some wind directions occurring more frequently in certain seasons. Therefore, top-down NO<sub>x</sub> emission estimates derived from several wind directions for a particular source, though sampled throughout all months, can vary depending on the seasonal influence on the observed TCNO<sub>2</sub> for which the wind direction more frequently occurs in. The top-down emissions derived here suggest that the NAEI bottom-up emissions for the largest sources such as London, Manchester and Birmingham are underestimated. The top-down emissions for London, Manchester and Birmingham are 49.2 (32.8, 65.9) moles/s, 19.7 (12.2, 27.3) moles/s and 21.0, 13.6, 28.6) moles/s with corresponding NAEI emissions of 32.7 moles, 10.6 moles/s and 14.7 moles/s, respectively. Note for Birmingham though, the NAEI emissions value sits within the top-down estimate uncertainty range.

For the smaller sources (e.g. Edinburgh, Bristol and Norwich), the comparisons are in better agreement with the NAEI and are located within the top-down emission ranges. However, for Newcastle the NAEI emissions (4.0 moles/s) are substantially larger than the top-down estimate (1.9 (0.8, 2.9) moles/s). In contrast, for Leeds (3.5 moles/s) and Glasgow (5.5 moles), the NAEI substantially underestimates the top-down emissions of 5.50 (3.6, 7.5) moles/s and 9.4 (5.8, 13.8) moles/s, respectively. For several of the top-down estimates under 10.0 moles/s, the NO<sub>2</sub> effective lifetime ranges between 1.75 and 3.5 hours. These lifetimes are at the lower range of expected values (Schaub et al., 2007; Pope et al., 2015), which in turn may yield positively skewed top-down estimates (e.g. Leeds and Glasgow). For all cities in **Figure 5** there is a strong correlation (0.99) between the NAEI and top-down emission sources investigated here, but the NAEI has a low bias of 2.95 moles/s (28.3%) on average, dominated by the larger sources (i.e. London, Manchester and Birmingham). These metrics were calculated in linear space.



### 3.4 Comparison of GEOS-Chem and Observation NO<sub>2</sub>

As the input emissions for GEOS-Chem come from the NAEI (2016 NAEI emissions scaled to 2019), any inconsistencies between simulated and observed NO<sub>2</sub> potentially indicates discrepancies in the underlying emissions. Such emission discrepancies, inferred by the model, and consistent with top-down – NAEI NO<sub>x</sub> emission differences would help act as a verification of the top-down emissions. **Figure 6** represents comparisons between GEOS-Chem and TROPOMI TCNO<sub>2</sub> between January and June 2019. In the case of London, there is a clear model underestimation of over  $3.0 \times 10^{-5}$  moles/m<sup>2</sup> and the green polygon-outlined region shows where the absolute bias lies outside the satellite uncertainty range. A similar substantial negative bias ( $-2.0$  to  $-1.0 \times 10^{-5}$  moles/m<sup>2</sup>) is found over Manchester. This suggests that the model, driven by the NAEI, substantially underestimates TROPOMI and that therefore the input emissions may be too low. For Birmingham, the GEOS-Chem-TROPOMI TCNO<sub>2</sub> biases are smaller peaking at  $-0.25 \times 10^{-5}$  moles/m<sup>2</sup>.

However, over some regions comparisons with TROPOMI show model positive biases ( $\sim 1.0$ – $2.0 \times 10^{-5}$  moles/m<sup>2</sup>). Investigation of January only shows that modelled TCNO<sub>2</sub> is substantially larger than TROPOMI across most of the central and north-eastern England. This is potentially suggestive of issues in the model's representation of the winter-time boundary layer where too much NO<sub>2</sub> is trapped (not shown here). When January is removed from the 2019 average, a larger negative GEOS-Chem-TROPOMI TCNO<sub>2</sub> bias is produced over Birmingham ( $-0.5 \times 10^{-5}$  moles/m<sup>2</sup>). Therefore, this again suggests that the NAEI NO<sub>x</sub> emissions may be too low when compared to the top-down estimate here.

We also compared GEOS-Chem with surface AURN NO<sub>2</sub> data from sites across the UK and subsampled to 13:00 LST each day to match the TROPOMI overpass and model output times, between January and June 2019. On average, there is a UK negative model-AURN bias of  $-9.96 \mu\text{g}/\text{m}^3$ . A substantial proportion of the bias will be the comparison of area-weighted model surface NO<sub>2</sub> against point measurement NO<sub>2</sub> observations. Here, the model horizontal resolution is too coarse to adequately represent smaller NO<sub>2</sub> sources (i.e. roads and point industry sources), while the AURN point measurements will be heavily influenced by higher resolution sources (Savage et al., 2013). AURN NO<sub>2</sub> measurements also use the chemiluminescence technique with molybdenum converters, which may overestimate true NO<sub>2</sub> concentrations and thus further compound the model negative bias (Savage et al., 2013 and references therein). When we compare the model against AURN for London, Birmingham and Manchester (averaging AURN sites within the city domains listed in **Table 1**) we find model biases of  $-15.3 \mu\text{g}/\text{m}^3$ ,  $-8.1 \mu\text{g}/\text{m}^3$  and  $19.0 \mu\text{g}/\text{m}^3$ , respectively. Unfortunately, all the other cities in **Figure 5** are limited to one AURN site at most. Therefore, one site is unlikely to be representative of city-scale NO<sub>2</sub> level and thus our analysis is limited to these three large cities. Overall, the model-AURN NO<sub>2</sub> negative biases at London and Manchester are larger than the UK average negative bias, and support our hypothesis that the NAEI NO<sub>x</sub> emissions are underestimated for London and Manchester. The model negative bias at Birmingham is of similar size to the UK average and thus suggestive that the NAEI NO<sub>x</sub> emissions over Birmingham are more reasonable.



#### 4. Conclusions

We have evaluated relationships between satellite observations (TROPOspheric Monitoring Instrument, TROPOMI) of tropospheric column nitrogen dioxide (TCNO<sub>2</sub>) and the UK National Atmospheric Emissions Inventory (NAEI) for nitrogen oxides (NO<sub>x</sub> = NO + NO<sub>2</sub>). Although they are different quantities, the short NO<sub>2</sub> lifetime means that our comparison can serve as a useful and important tool to evaluate bottom-up emissions. Here, spatial comparison of the TROPOMI TCNO<sub>2</sub> with the NAEI highlights consistency over the source regions with co-located peak values in the respective data sets. Correlation analysis of TCNO<sub>2</sub> and NO<sub>x</sub> emissions over the UK cities indicates moderate spatial agreement with R ranging between 0.4 and 0.6 (significant at the >90% confidence level). Analysis of long-term satellite records of TCNO<sub>2</sub> (from the Ozone Monitoring Instrument (OMI), 2005–2015) show comparable negative trends with the NAEI NO<sub>x</sub> emissions with rates of -2.2%/yr and -4.4%/yr, respectively. Though the relative NAEI trend is larger than OMI, meteorological conditions and photochemistry will control the atmospheric response to a change in NO<sub>x</sub> emissions, as seen by OMI. It is also possible that the NAEI overestimates the decreasing NO<sub>x</sub> emissions trend.

We have also used TROPOMI data to derive top-down city-scale estimates of UK NO<sub>x</sub> emissions. While it can still be challenging to derive emissions from moderately sized sources (e.g. cities such as Bristol and Cardiff), we estimate top-down emissions fluxes (using satellite data between February 2018 and January 2020) for larger sources (i.e. London and Manchester) and find values substantially larger than those in the NAEI for 2019 (i.e. 2016 emissions scaled to 2019). When these NAEI emissions are used to drive the GEOS-Chem atmospheric chemistry model, we find substantial negative biases between the model and satellite/surface observations for London and Manchester. Therefore, this provides further evidence that the NAEI emissions for London and Manchester may be underestimated. Other sources, with lower emission rates (e.g. below 10.0 moles/s), tend to be in reasonable agreement between both datasets (i.e. NAEI emission rate is within the top-down emission uncertainty range).

Overall, as far as we are aware, this study represents the first attempt to use satellite observations of TCNO<sub>2</sub> to evaluate and constrain the official UK bottom-up NAEI. We find spatial and temporal agreement between the two quantities, but find evidence that the NAEI NO<sub>x</sub> emissions for larger sources (e.g. London) may be too low (i.e. >25%) sitting outside the top-down emission uncertainty ranges (i.e. based on the satellite retrieval errors). To fully understand the discrepancies and the drivers of these NO<sub>x</sub> emissions differences, further investigation is required.

#### Data Availability

TROPOMI and OMI tropospheric column NO<sub>2</sub> data comes from the Tropospheric Emissions Monitoring Internet Service (TEMIS, <http://www.temis.nl/airpollution/no2.html>). The bottom-up NO<sub>x</sub> emissions come from the National Atmospheric Emissions Inventory (<https://naei.beis.gov.uk/data/data-selector?view=air-pollutants>) and the point and area sources can be obtained from [https://naei.beis.gov.uk/data/map-uk-das?pollutant\\_id=6&emiss\\_maps\\_submit=naei-20210325121854](https://naei.beis.gov.uk/data/map-uk-das?pollutant_id=6&emiss_maps_submit=naei-20210325121854). The specific UK total NO<sub>x</sub> emissions came from <https://naei.beis.gov.uk/data/data-selector-results?q=142818>. Meteorological wind data came from ECMWF



(<https://cds.climate.copernicus.eu/cdsapp#!/dataset/reanalysis-era5-pressure-levels?tab=overview>). The AURN data was obtained from <https://uk-air.defra.gov.uk/networks/network-info?view=aurn>.

#### Author contribution

RJP undertook the research looking at the spatial maps and long-term trends. RJP, RK, CW and AMG worked on the satellite top-down city-scale NO<sub>x</sub> emission estimates. EAM provided the GEOS-Chem simulations. RJP prepared the manuscript with contributions from all co-authors.

#### Competing interests

The authors declare that they have no conflict of interest.

#### Acknowledgements

This work was funded by the Department for Environment, Food and Rural Affairs Affairs through the “Applying Earth Observation (EO) to Reduce Uncertainties in Emission Inventories” project and by the UK Natural Environment Research Council (NERC) by providing funding for the National Centre for Earth Observation (NCEO, award reference NE/R016518/1).

#### References

- AURN. Automated Urban and Rural Network [Online]. Available: <https://uk-air.defra.gov.uk/networks/network-info?view=aurn> (accessed 30<sup>th</sup> March 2021), 2021.
- Beirle, S., Boersma, B.F., Platt, U., Lawrence, M.G. and Wagner, T.: Megacity emissions and lifetimes of nitrogen oxides probed from space, *Science*, 333, 1737, doi:10.1126/science.1207824, 2011.
- Boersma, K.F., Eskes, H.J., Veeffkind, J.P., Brinksma, E.J., van der A, R.J., Sneep, M., van den Oord, G.H.J., Levelt, P.F., Stammes, P., Gleason, J.F. and Bucsela, E.J.: Near-real time retrieval of tropospheric NO<sub>2</sub> from OMI, *Atmospheric Chemistry and Physics*, 7, 2103–2118, doi:10.5194/acp-7-2103-2007, 2007.
- Braak R. 2010. Row Anomaly Flagging Rules Lookup Table, KNMI Technical Document TN-OMIE-KNMI-950, *KNMI*, Netherlands.
- Chan, K. L., Wiegner, M., van Geffen, J., De Smedt, I., Alberti, C., Cheng, Z., Ye, S. and Wenig, M.: MAX-DOAS measurements of tropospheric NO<sub>2</sub> and HCHO in Munich and the comparison to OMI and TROPOMI satellite observations, *Atmospheric Measurement Techniques*, 13, 4499–4520, doi: 10.5194/amt-13-4499-2020, 2020.
- DEFRA. Air Pollution in the UK 2017 [Online]. Available: [https://uk-air.defra.gov.uk/assets/documents/annualreport/air\\_pollution\\_uk\\_2017\\_issue\\_1.pdf](https://uk-air.defra.gov.uk/assets/documents/annualreport/air_pollution_uk_2017_issue_1.pdf) (last accessed 30<sup>th</sup> March 2021), 2018a.
- DEFRA. UK Informative Inventory Report (1990 to 2016) [Online]. Available: [https://uk-air.defra.gov.uk/library/reports?report\\_id=956](https://uk-air.defra.gov.uk/library/reports?report_id=956) (last accessed 30<sup>th</sup> March 2021), 2018b.
- DEFRA. Air Pollution in the UK 2019 [Online]. Available: [https://uk-air.defra.gov.uk/library/annualreport/viewonline?year=2019\\_issue\\_1#report\\_pdf](https://uk-air.defra.gov.uk/library/annualreport/viewonline?year=2019_issue_1#report_pdf) (accessed 30<sup>th</sup> March 2021), 2020.



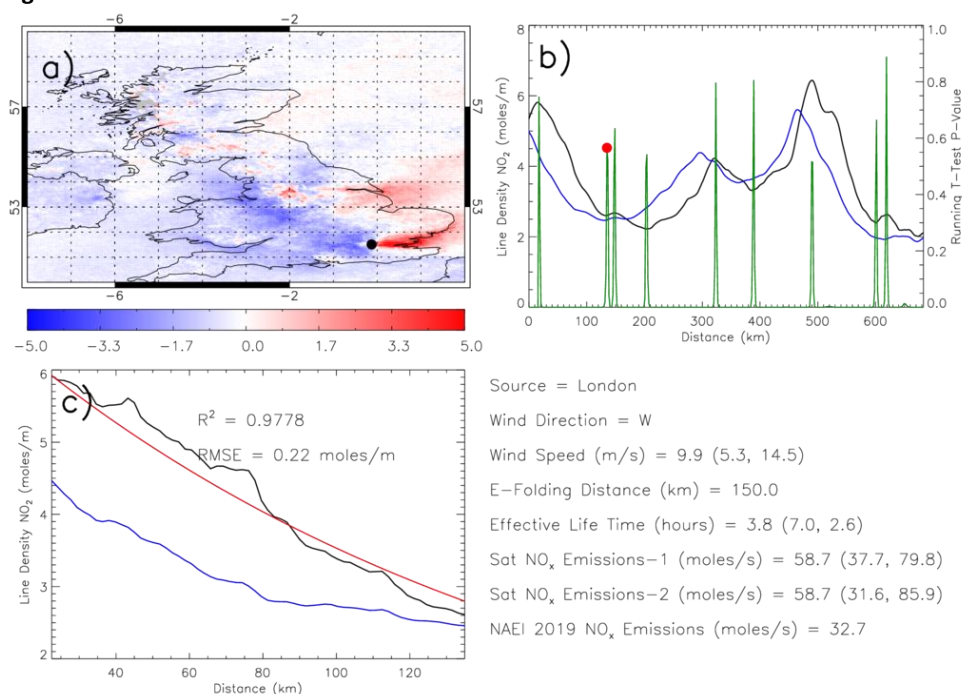
- 558 Dibbenn, C. and Clemens, T.: Place of work and residential exposure to ambient air pollution  
 559 and birth outcomes in Scotland, using geographically fine pollution climate mapping  
 560 estimates, *Environmental Research*, 140, 535–541, doi:10.1016/j.envres.2015.05.010,  
 561 (2015).
- 562 Dimitropoulou, E., Hendrick, F., Pinardi, G., Friedrich, M. M., Merlaud, A., Tack, F., De  
 563 Lougeville, H., Fayt, C., Hermans, C., Laffineur, Q., Fierens, F. and Van Roozendaal, M.:  
 564 Validation of TROPOMI tropospheric NO<sub>2</sub> columns using dual-scan multi-axis differential  
 565 optical absorption spectroscopy (MAX-DOAS) measurements in Uccle, Brussels, *Atmospheric*  
 566 *Measurement Techniques*, 13, 5165–5191, doi: 10.5194/amt-13-5165-2020, 2020.
- 567 EEA. Air quality in Europe — 2018 report [Online]. Available:  
 568 <https://www.eea.europa.eu/publications/air-quality-in-europe-2018> (accessed 30<sup>th</sup> March  
 569 2021), 2018.
- 570 EMEP/EEA. EMEP/EEA air pollutant emission inventory guidebook 2019, EEA Report No  
 571 13/2019, ISSN 1977-8449. Available: [https://www.eea.europa.eu/publications/emep-eea-](https://www.eea.europa.eu/publications/emep-eea-guidebook-2019)  
 572 [guidebook-2019](https://www.eea.europa.eu/publications/emep-eea-guidebook-2019) (accessed 2<sup>nd</sup> July 2021), 2019.
- 573  
 574 EMEP. EMEP – Convention on Long-range Transboundary Air Pollution. Available:  
 575 <https://www.emep.int/> (accessed 12<sup>th</sup> July 2021), 2021.
- 576  
 577 Liu, F., Beirle, S., Zhang, Q., Dörner, S., He, K. and Wagner T.: NO<sub>x</sub> lifetimes and emissions of  
 578 cities and power plants in polluted background estimated by satellite observations,  
 579 *Atmospheric Chemistry and Physics*, 16, 5283–5298, doi:10.5194/acp-16-5283-2016, 2016.
- 580 Martin, R.V., Jacob, D.J., Chance, K., Kurosu, T.P., Palmer, P.I. and Evans, M.J.: Global  
 581 inventory of nitrogen oxide emissions constrained by space-based observations of NO<sub>2</sub>  
 582 columns, *Journal of Geophysical Research*, 108, 4537, doi:10.1029/2003JD003453, 2003.
- 583 Miyazaki, K., Eskes, H., Sudo, K., Boersma, K.F., Bowman, K. and Kanaya, Y.: Decadal changes  
 584 in global surface NO<sub>x</sub> emissions from multi-consistent satellite data assimilation,  
 585 *Atmospheric Chemistry and Physics*, 17, 807–837, doi:10.5194/acp-17-807-2017, 2016.
- 586 NAEI. UK Emission Mapping Methodology. – 2015 [Online]. Available: [https://uk-](https://uk-air.defra.gov.uk/assets/documents/reports/cat07/1710261436_Methodology_for_NAEI_2017.pdf)  
 587 [air.defra.gov.uk/assets/documents/reports/cat07/1710261436\\_Methodology\\_for\\_NAEI\\_20](https://uk-air.defra.gov.uk/assets/documents/reports/cat07/1710261436_Methodology_for_NAEI_2017.pdf)  
 588 [17.pdf](https://uk-air.defra.gov.uk/assets/documents/reports/cat07/1710261436_Methodology_for_NAEI_2017.pdf) (accessed 30<sup>th</sup> March 2021), 2017.
- 589 NAEI. UK-NAEI – National Atmospheric Emissions Inventory [Online]. Available:  
 590 <https://naei.beis.gov.uk/> (accessed 30<sup>th</sup> March 2021), 2021.
- 591 Pope, R.J., Savage, N.H., Chipperfield, M.P., Ordonez, C. and Neal, L.S.: The influence of  
 592 synoptic weather regimes on UK air quality: Regional model studies of tropospheric column  
 593 NO<sub>2</sub>, *Atmospheric Chemistry and Physics*, 15, 11201–11215, doi:10.5194/acp-15-11201-  
 594 2015, 2015.
- 595 Pope, R.J., Arnold, S.R., Chipperfield, M.P., Latter, B.G., Siddans, R. and Kerridge, B.J.:  
 596 Widespread changes in UK air quality observed from space, *Atmospheric Science Letters*, 19,  
 597 e817, doi: 10.1002/asl.817, 2018.
- 598 Potts, D.A., Marais, E.A., Boesch, H., Pope, R.J., Lee, J., Drysdale, W., Chipperfield, M.P.,  
 599 Kerridge, B. and Siddans, R.: Diagnosing air quality changes in the UK during the COVID-19



- lockdown using TROPOMI and GEOS-Chem, *Environmental Research Letters*, 16, 054031, doi:10.1088/1748-9326/abde5d, 2021.
- Ricardo Energy and Environment. UK Informative Inventory Report (1990 to 2019). Available: [https://uk-air.defra.gov.uk/assets/documents/reports/cat09/2103151107\\_GB\\_IIR\\_2021\\_FINAL.pdf](https://uk-air.defra.gov.uk/assets/documents/reports/cat09/2103151107_GB_IIR_2021_FINAL.pdf) (accessed 2<sup>nd</sup> July 2021), 2021.
- Royal College of Physicians. Every breath we take: the lifelong impact of air pollution [Online]. Available: <https://www.rcplondon.ac.uk/projects/outputs/every-breath-we-take-lifelong-impact-air-pollution> (accessed 30<sup>th</sup> March 2021), 2016.
- Savage, N.H., Agnew, P., Davis, L.S., Ordóñez, C., Thorpe, R., Johnson, C.E., O'Connor, F.M. and Dalvi, M.: Air quality modelling using the Met Office Unified Model (AQUUM OS24-26): model description and initial evaluation, *Geoscientific Model Development*, 6, 353–372, doi:10.5194/gmd-6-353-2013, 2013.
- Schaub, D., Brunner, D., Boersma, K.F., Keller, J., Folini, D., Buchmann, B., Berresheim, H. and Staehelin, J.: SCIAMACHY tropospheric NO<sub>2</sub> over Switzerland: estimates of NO<sub>x</sub> lifetime and impacts of the complex alpine topography on the retrieval, *Atmospheric Chemistry and Physics*, 7, 5971–5987, doi:10.5194/acp-7-5971-2007, 2007.
- Seinfeld, J. and Pandis, S.: Atmospheric Chemistry and Physics: From Air Pollution to Climate Change - Second Edition, John Wiley and Sons Inc, New Jersey, USA, 2006.
- UK Government. The Environmental Permitting (England and Wales) Regulations 2016. Available: <https://www.legislation.gov.uk/ukxi/2016/1154/contents/made> (last accessed 2<sup>nd</sup> July 2021), 2016.
- Veefkind, J.P., Aben, I., McMullan, K., Forster, H., de Vries, J., Otter, G., Claas, J., Eskes, H.J., de Haan, F., Kleipool, Q., van Weele, M., Hasekamp, O., Hoogeveen, R., Landgraf, J., Snel, R., Tol, P., Ingmann, P., Voors, R., Kruizinga, B., Vink, R., Visser, H. and Levelt, P.F.: TROPOMI on the ESA Sentinel-5 Precursor: A GMES mission for global observations of atmospheric composition for climate, air quality and ozone layer applications, *Remote Sensing of Environment*, 120, 70–83, doi:10.1016/j.rse.2011.09.027, 2012.
- Verhoelst, T., Compernelle, S., Pinardi, G., Lambert, J. C., Eskes, H., Eichmann, K. U., et al.: Ground-based validation of the Copernicus Sentinel-5P TROPOMI NO<sub>2</sub> measurements with the NDACC ZSL-DOAS, MAX-DOAS and Pandonia global networks, *Atmospheric Measurement Techniques*, 14, 481–510, doi: 10.5194/amt-14-481-2021, 2021.
- Verstraeten, W.W., Boersma, K.F., Douros, J., Williams, J.E., Eskes, H., Liu, F., Beirle, S. and Delcloo, A.: Top-down NO<sub>x</sub> emissions of European cities based on the downwind plume of modelled and space-borne tropospheric NO<sub>2</sub> column, *Sensors*, 18 (9), 2893, doi:10.3390/s18092893, 2018.
- WHO. Ambient (outdoor) air pollution [Online]. Available: [https://www.who.int/news-room/fact-sheets/detail/ambient-\(outdoor\)-air-quality-and-health](https://www.who.int/news-room/fact-sheets/detail/ambient-(outdoor)-air-quality-and-health) (last accessed 30<sup>th</sup> March 2021), 2018.
- Wu, H., Reis, S., Lin, C. and Heal, M.R.: Effect of monitoring network design on land use regression models for estimating residential NO<sub>2</sub> concentration, *Atmospheric Environment*, 149, 24–33, doi:10.1016/j.atmosenv.2016.11.014, 2017.

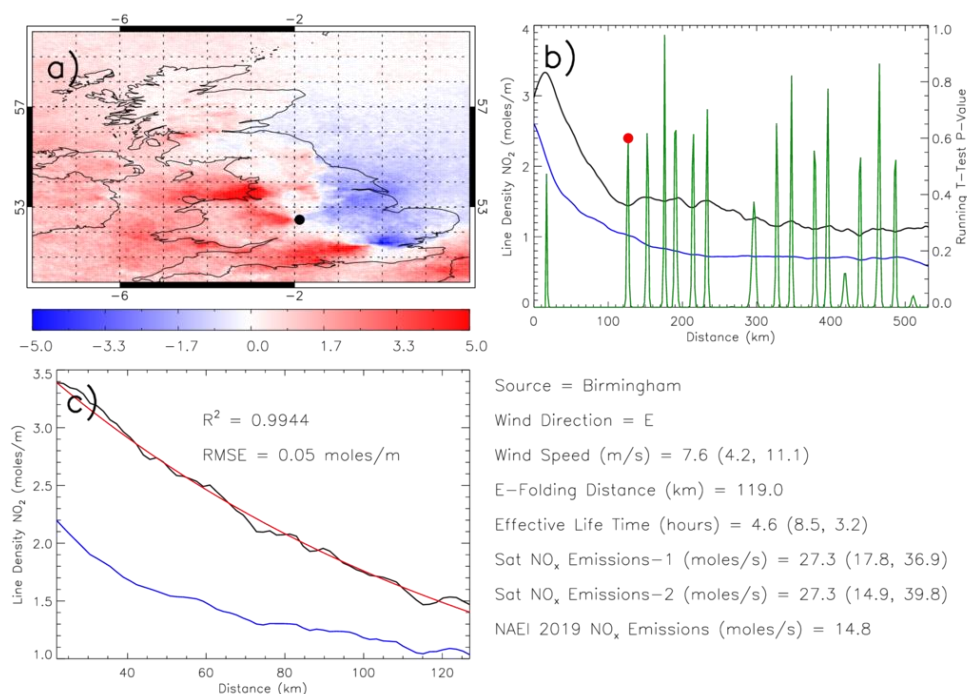


# Figures



643

644 **Figure 1:** (a) TCNO<sub>2</sub> (10<sup>-5</sup> moles/m<sup>2</sup>) sub-sampled under westerly flow (defined over London,  
 645 black dot) minus the long-term average. (b) Downwind NO<sub>2</sub> LD from London (black =  
 646 westerly flow, blue = all-flow average) with the corresponding running t-test p-value (green  
 647 line). The red dot represents the location of background level determined by the turning  
 648 point in the running t-test p-value time series. (c) The westerly flow and all-flow NO<sub>2</sub> LD  
 649 between peak westerly flow NO<sub>2</sub> LD and the background value. The red line represents the e-  
 650 folding distance fit with the corresponding R<sup>2</sup> and root mean square error (RMSE) between  
 651 the westerly flow NO<sub>2</sub> LD and fit profile.



652

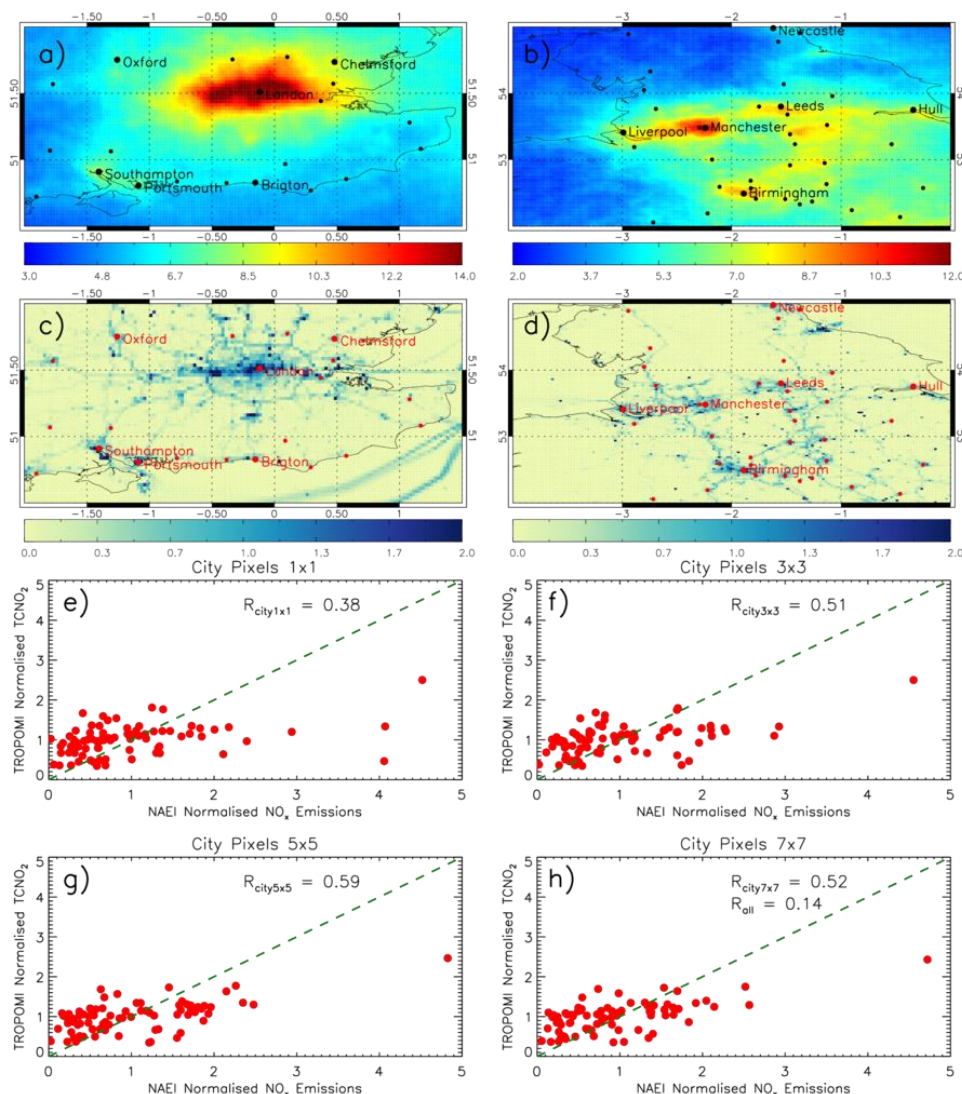
653 **Figure 2:** (a) TCNO<sub>2</sub> ( $10^{-5}$  moles/m<sup>2</sup>) sub-sampled under easterly flow (defined over  
 654 Birmingham, black dot) minus the long-term average. (b) Downwind NO<sub>2</sub> LD from  
 655 Birmingham (black = easterly flow, blue = all-flow average) with the corresponding running  
 656 t-test p-value (green line). The red dot represents the location of background level  
 657 determined by the turning point in the running t-test p-value time series. (c) The easterly  
 658 flow and all-flow NO<sub>2</sub> LD between peak easterly flow NO<sub>2</sub> LD and the background value. The  
 659 red line represents the e-folding distance fit with the corresponding R<sup>2</sup> and root mean square  
 660 error (RMSE) between the easterly flow NO<sub>2</sub> LD and fit profiles.

661

662



663



664

665

666 **Figure 3:** TROPOMI TCNO<sub>2</sub> (×10<sup>-5</sup> moles/m<sup>2</sup>) average for February 2018 to January 2020  
 667 across (a) south-eastern and (b) northern England. Black circles represent city locations. NAEI  
 668 NO<sub>x</sub> emissions (μg/m<sup>2</sup>/s) for 2016 across (c) south-eastern and (d) northern England. Red  
 669 circles represent city locations. Panels (e)-(h) represent the correlation of normalised TCNO<sub>2</sub>  
 670 and NO<sub>x</sub> emissions for UK cities. The green dashed line is the 1:1 line. Each source is  
 671 normalised by the average of all the sources. The four panels also represent city means using  
 672 varying pixel ranges around the source (i.e. 1x1, 3x3, 5x5 and 7x7 grid pixels). The  
 673 correlations between the city-scale normalised NO<sub>x</sub> emissions and TCNO<sub>2</sub> are shown (R).  
 674

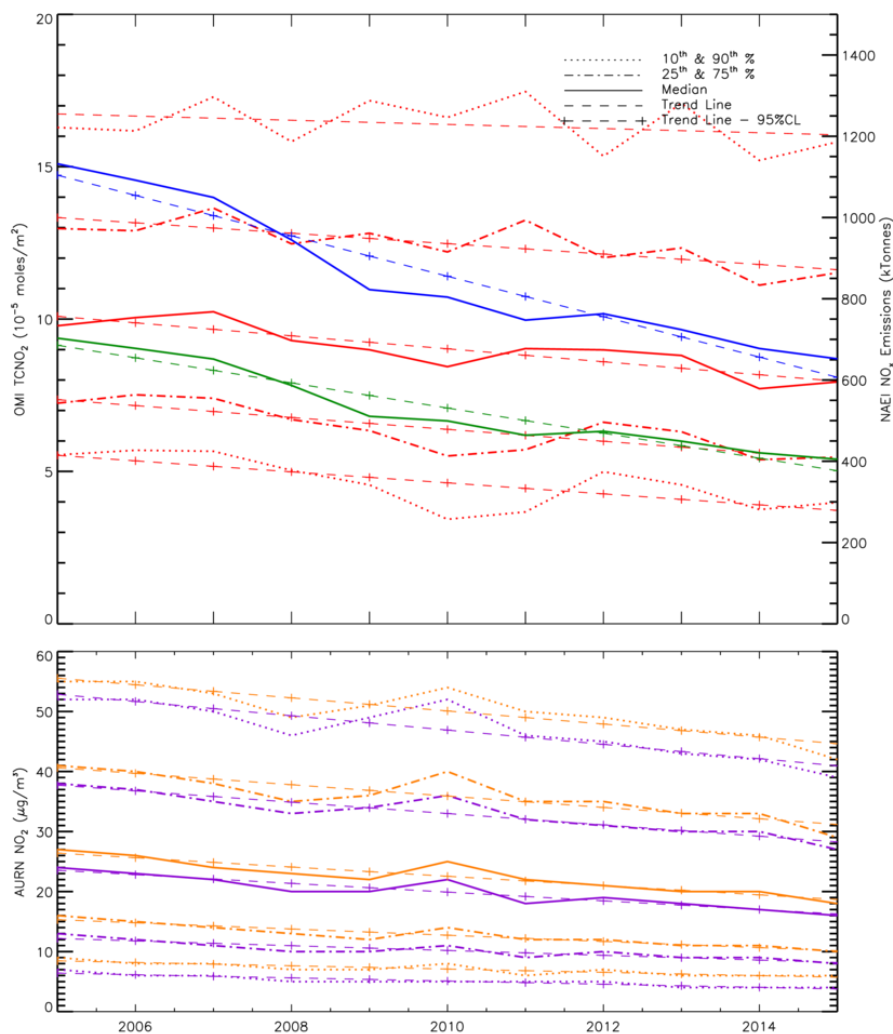
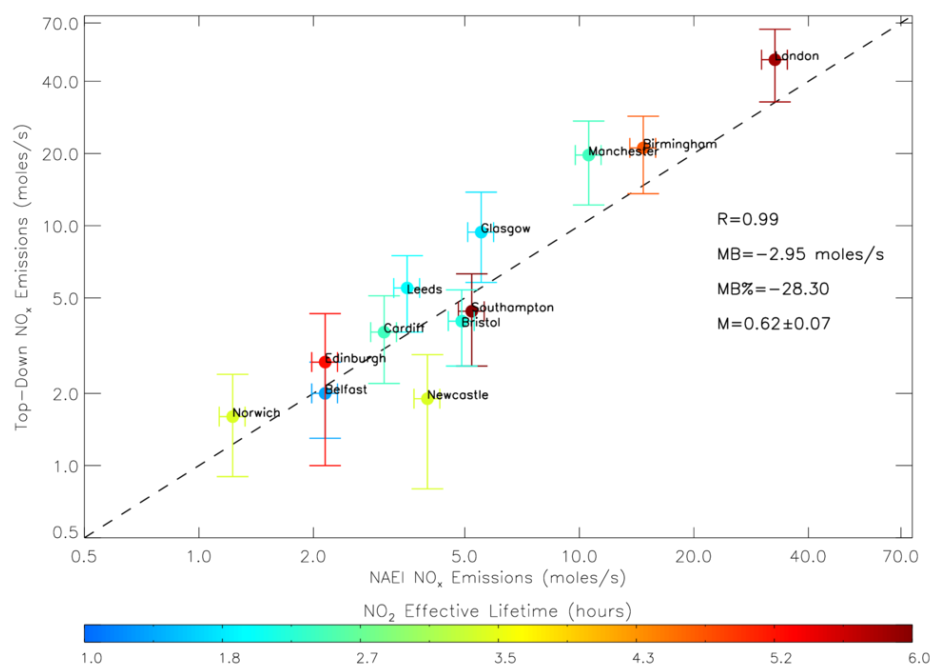


**Figure 4:** Trends in OMI TCNO<sub>2</sub> ( $\times 10^{-5}$  moles/m<sup>2</sup>, red lines). NAEI NO<sub>x</sub> emission (kt or Gg) trends are shown for the UK (blue) and England (green) (top panel). AURN surface NO<sub>2</sub> ( $\mu\text{g}/\text{m}^3$ ) trends are shown for the UK (purple) and England (orange) (bottom panel). Significant trends at the 95% confidence level are shown with crosses.



682

683

**Figure 5:** NAEI and top-down  $\text{NO}_x$  emissions (moles/s) for 12 UK cities coloured by the  $\text{NO}_2$  effective lifetime (hours). The correlation ( $R$ ), mean bias ( $MB$ , moles/s), percentage mean bias ( $MB\%$ ) and linear fit ( $M$ ) are also shown. NAEI uncertainty is  $\pm 7.8\%$  (DEFRA, 2018b) and the top-down uncertainty range is based on satellite errors (i.e. Sat Emissions-1, see text). The black dashed line represents the 1:1 relationship and both axes are on log scales.

687

688

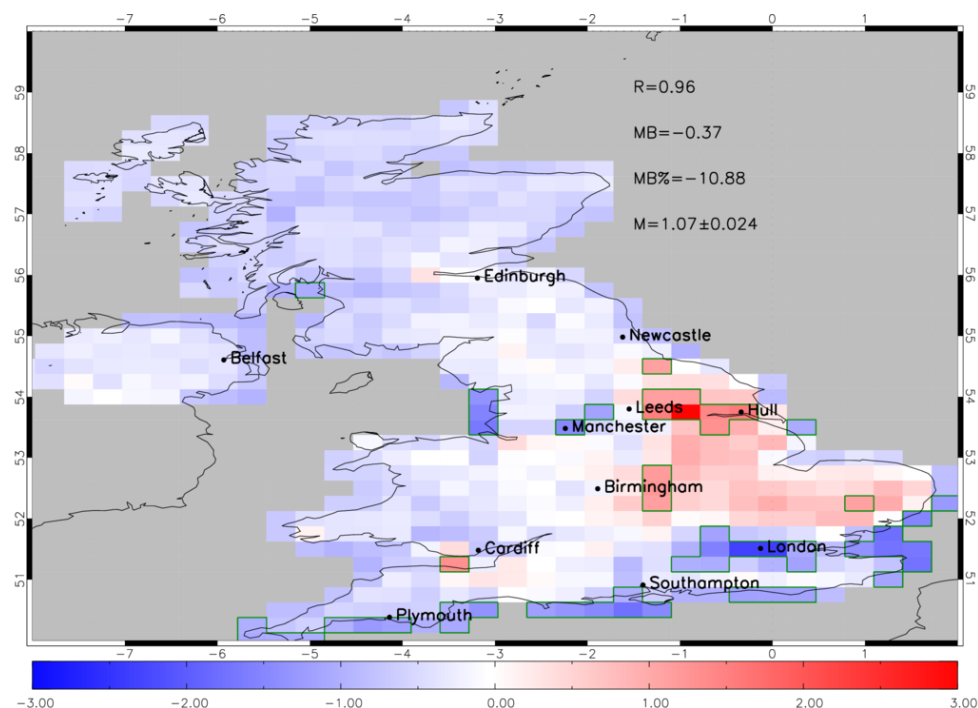


**Figure 6:** GEOS-Chem minus TROPOMI mean  $\text{TCNO}_2$  ( $10^{-5}$  moles/ $\text{m}^2$ ) for January to June 2019. The green polygon-outlined regions represent where the absolute model-satellite bias is greater than the satellite error (i.e.  $|\text{mod-sat}| > \text{sat error}$ ) and the absolute bias ( $|\text{mod-sat}|$ ) is greater than  $1.0 \times 10^{-5}$  moles/ $\text{m}^2$  (i.e. where biases are the same order of magnitude as the mean  $\text{TCNO}_2$  state). The domain correlation ( $R$ ), mean bias ( $MB$ ), percentage mean bias ( $MB\%$ ) and linear fit ( $M$ ) are shown.



**Table 1:** List of top-down  $\text{NO}_x$  (moles/s) emission estimates for UK city sources under different wind directions. Sat  $\text{NO}_x$  Emissions-1 represents the emission flux estimated using the TROPOMI  $\text{NO}_2 \pm$  the retrieval uncertainty, while Sat  $\text{NO}_x$  Emissions-2 is based on the lifetime derived from the wind speed data  $\pm 1.0$  sigma standard deviation.

Source Name	London	London	London	Glasgow
Longitude	-0.13	-0.13	-0.13	-4.28
Latitude	51.51	51.51	51.51	55.86
Lon Edge - West	-0.52	-0.52	-0.52	-4.47
Lon Edge - East	0.28	0.28	0.28	-4.07
Lat Edge - South	51.32	51.32	51.32	55.78
Lat Edge - North	51.69	51.69	51.69	55.93
Wind Speed Average (m/s)	9.90	7.10	7.50	9.50
Wind Speed Standard Deviation (m/s)	4.60	3.40	3.50	4.80
Wind Direction	W	N	E	S
E-Folding Distance (km)	150.00	197.00	203.00	71.00
Life Time (hr)	3.80	8.30	5.30	1.30
Life Time- Lower Wind (hr)	7.00	16.20	10.10	2.60
Life Time- Upper Wind (hr)	2.60	5.60	3.60	0.90
Satellite Emission Rate (moles/s)	58.70	52.50	36.60	7.50
Sat $\text{NO}_x$ Emissions-1 - Lower (moles/s)	37.70	35.20	25.40	4.40
Sat $\text{NO}_x$ Emissions-1 - Upper (moles/s)	79.80	69.90	47.90	10.60
Sat $\text{NO}_x$ Emissions-2 - Lower (moles/s)	31.60	26.90	19.30	3.80
Sat $\text{NO}_x$ Emissions-2 - Upper (moles/s)	85.90	78.10	54.00	11.30
NAEI Emission Rate (moles/s)	32.70	32.70	32.70	5.50

719

Source Name	Glasgow	Birmingham	Birmingham	Birmingham
Longitude	-4.28	-1.89	-1.89	-1.89
Latitude	55.86	52.50	52.50	52.50
Lon Edge - West	-4.47	-2.18	-2.18	-2.18
Lon Edge - East	-4.07	-1.72	-1.72	-1.72
Lat Edge - South	55.78	52.35	52.35	52.35
Lat Edge - North	55.93	52.66	52.66	52.66
Wind Speed Average (m/s)	8.50	7.60	5.90	9.70
Wind Speed Standard Deviation (m/s)	4.40	3.40	2.70	5.50
Wind Direction	E	E	N	S
E-Folding Distance (km)	75.00	119.00	177.00	117.00
Life Time (hr)	2.20	4.60	7.20	2.20
Life Time- Lower Wind (hr)	4.60	8.50	13.50	5.10
Life Time- Upper Wind (hr)	1.50	3.20	4.90	1.40
Satellite Emission Rate (moles/s)	11.20	27.30	13.90	22.10
Sat $\text{NO}_x$ Emissions-1 - Lower (moles/s)	7.10	17.80	8.90	14.00
Sat $\text{NO}_x$ Emissions-1 - Upper (moles/s)	15.40	36.90	18.80	30.20
Sat $\text{NO}_x$ Emissions-2 - Lower (moles/s)	5.50	14.90	7.40	9.60
Sat $\text{NO}_x$ Emissions-2 - Upper (moles/s)	17.00	39.80	20.30	34.60
NAEI Emission Rate (moles/s)	5.50	14.80	14.80	14.80

720



721

Source Name	Newcastle	Southampton	Manchester	Manchester
Longitude	-1.62	-1.41	-2.25	-2.25
Latitude	54.98	50.92	53.50	53.50
Lon Edge - West	-1.73	-1.49	-2.47	-2.47
Lon Edge - East	-1.40	-1.32	-2.01	-2.01
Lat Edge - South	54.92	50.88	53.37	53.37
Lat Edge - North	55.02	50.95	53.60	53.60
Wind Speed Average (m/s)	10.60	6.80	5.80	9.50
Wind Speed Standard Deviation (m/s)	4.80	3.20	2.90	4.00
Wind Direction	W	N	N	W
E-Folding Distance (km)	239.00	250.00	97.00	32.00
Life Time (hr)	3.40	9.00	3.90	0.90
Life Time- Lower Wind (hr)	6.10	16.90	7.80	1.60
Life Time- Upper Wind (hr)	2.30	6.10	2.60	0.70
Satellite Emission Rate (moles/s)	1.90	4.40	13.40	26.0
Sat NOx Emissions-1 - Lower (moles/s)	0.80	2.60	8.50	15.80
Sat NOx Emissions-1 - Upper (moles/s)	2.90	6.30	18.30	36.20
Sat NOx Emissions-2 - Lower (moles/s)	1.00	2.40	6.60	15.10
Sat NOx Emissions-2 - Upper (moles/s)	2.70	6.50	20.20	36.90
NAEI Emission Rate (moles/s)	4.00	5.20	10.60	10.60

722

Source Name	Belfast	Edinburgh	Norwich	Cardiff
Longitude	-5.93	-3.19	1.29	-3.18
Latitude	54.61	55.96	52.63	51.49
Lon Edge - West	-6.00	-3.32	1.20	-3.36
Lon Edge - East	-5.84	-3.10	1.38	-3.10
Lat Edge - South	54.55	55.89	52.60	51.45
Lat Edge - North	54.70	55.98	52.69	51.55
Wind Speed Average (m/s)	8.60	10.80	10.10	5.70
Wind Speed Standard Deviation (m/s)	4.20	4.50	5.20	2.60
Wind Direction	E	W	W	N
E-Folding Distance (km)	83.00	229.00	267.00	64.00
Life Time (hr)	1.40	5.20	3.40	2.40
Life Time- Lower Wind (hr)	2.80	9.00	6.90	4.50
Life Time- Upper Wind (hr)	0.90	3.60	2.20	1.70
Satellite Emission Rate (moles/s)	2.00	2.70	1.60	3.60
Sat NOx Emissions-1 - Lower (moles/s)	1.30	1.00	0.90	2.20
Sat NOx Emissions-1 - Upper (moles/s)	2.70	4.30	2.40	5.10
Sat NOx Emissions-2 - Lower (moles/s)	1.00	1.50	0.80	2.00
Sat NOx Emissions-2 - Upper (moles/s)	3.0	3.80	2.50	5.20
NAEI Emission Rate (moles/s)	2.2	2.2	1.20	3.1

723

724

725

726



Source Name	Leeds	Leeds	Bristol
Longitude	-1.55	-1.55	-2.59
Latitude	53.80	53.80	51.46
Lon Edge - West	-1.69	-1.69	-2.74
Lon Edge - East	-1.44	-1.44	-2.47
Lat Edge - South	53.74	53.74	51.40
Lat Edge - North	53.86	53.86	51.55
Wind Speed Average (m/s)	8.60	9.50	7.30
Wind Speed Standard Deviation (m/s)	4.20	5.30	3.80
Wind Direction	E	S	E
E-Folding Distance (km)	50.00	189.00	108.00
Life Time (hr)	1.00	2.90	2.20
Life Time- Lower Wind (hr)	2.00	6.70	4.50
Life Time- Upper Wind (hr)	0.70	1.90	1.40
Satellite Emission Rate (moles/s)	3.40	7.60	4.00
Sat NOx Emissions-1 - Lower (moles/s)	2.20	4.90	2.60
Sat NOx Emissions-1 - Upper (moles/s)	4.50	10.40	5.40
Sat NOx Emissions-2 - Lower (moles/s)	1.70	3.40	1.90
Sat NOx Emissions-2 - Upper (moles/s)	5.00	11.90	6.10
NAEI Emission Rate (moles/s)	3.50	3.50	4.90

727

728

729